J|A|C|S
ARTICLES
Published on Web 11/12/2002

Three-Dimensional Structure Determination of *N*-(*p*-Tolyl)-dodecylsulfonamide from Powder Diffraction Data and Validation of Structure Using Solid-State NMR Spectroscopy

Manju Rajeswaran,*,† Thomas N. Blanton,† Nicholas Zumbulyadis,† David J. Giesen,† Carlota Conesa-Moratilla,‡ Scott T. Misture,§ Peter W. Stephens,|| and Ashfia Huq||

Contribution from the Research and Development Laboratories, Eastman Kodak Company, Rochester, New York 14650-2106, Accelrys, 230/250 The Quorum, Barnwell Road, Cambridge CB5 8RE, England, New York State College of Ceramics at Alfred University, Institute for Ceramic Superconductivity, Binns-Merrill Hall, Alfred, New York 14802, and Department of Physics and Astronomy, SUNY-Stony Brook, Stony Brook, New York 11794-3800

Received August 1, 2002

Abstract: The three-dimensional structure, conformation, and packing of molecules in the solid state are crucial components used in the optimization of many technologically useful materials properties. Single-crystal X-ray diffraction is the traditional and most effective method of determining 3-D structures in the solid state. Obtaining single crystals that are sufficiently large and free of imperfections is often laborious, time-consuming, and, occasionally, impossible. The feasibility of an integrated approach to the determination and verification of a complete three-dimensional structure for a medium-sized organic molecule without using single crystals is demonstrated for the case of an organic stabilizer compound *N*-(*p*-tolyl)-dodecylsulfonamide. The approach uses a combination of powder XRD data, several computational packages involving Monte Carlo simulations and ab initio quantum mechanical calculations, and experimental solid-state NMR chemical shifts. Structure elucidation of *N*-(*p*-tolyl)-dodecylsulfonamide revealed that the Bravais lattice is monoclinic, with cell dimensions of $a = 38.773$ Å, $b = 5.507$ Å, $c = 9.509$ Å, and $\beta = 86.35°$, and a space group of $P21/c$.

Introduction

The crystal structure of a material is the arrangement of atoms or molecules in the solid state. The crystal structure controls properties such as color, solubility, density, and stability and helps to explain why a material or chemical behaves in a certain way. Changing or controlling the crystal structure is one way of changing the properties of a system. The morphology of a crystal, which is related to the underlying structure, also affects many of these properties and impacts processing and formulations. Crystallization with subsequent plugging of chemical transfer lines can be a big problem in production areas. Crystallization on photographic paper can lead to light scattering on pictures. Knowledge of the crystal structure is the key in the design of additives that inhibit the growth of the most active crystal faces of crystals. Single-crystal X-ray diffraction continues to be the preferred method for solving crystal structures. However, this approach requires single crystals of sufficient size and quality. These crystals can be difficult to produce on demand, and it is often the case that crystallization experiments yield polycrystalline samples that must be analyzed using powder diffraction techniques. Determination and verification of a complete three-dimensional structure for a medium-sized organic molecule without using single crystals are demonstrated.

Background

Data collected using a sealed tube or rotating anode diffraction system often lack the resolution required to accurately define the number and diffraction angle of all diffraction peaks. These problems can be overcome by utilizing high-resolution diffraction data.[1]

As in single-crystal diffraction, indexing of the unit cell presents the biggest obstacle associated with crystal structure elucidation from powder diffraction data. The lattice parameters can be refined to confirm the indexing of all observed diffraction peaks. A number of techniques are available to index the diffraction pattern, allowing unit cell parameters to be derived.[2−5] It should be emphasized that if the indexing is incorrect or

* To whom correspondence should be addressed. E-mail: manju.rajeswaran@kodak.com.
† Eastman Kodak Company.
‡ Accelrys.
§ New York State College of Ceramics at Alfred University.
|| SUNY-Stony Brook.

(1) National Synchrotron Light Source 2000 Activity Report; http://www.pubs.bnl.gov/nsls00/pdf/blan7229.pdf.
(2) Visser, J. W. *J. Appl. Crystallogr.* **1969**, *2*, 89.
(3) Werner, P. E.; Eriksson, L.; Westdahl, M. *J. Appl. Crystallogr.* **1985**, *18*, 367.

10.1021/ja027978b CCC: $22.00

cannot be obtained, any additional activities involving crystal structure determination from powder diffraction data are futile.

Indexing is followed by Pawley refinement.[6] The main purpose of Pawley refinement is to provide peak profile parameters, background parameters, unit cell parameters, and the zero-point shift for the structure solution step. In addition, the correctness of the indexing result is easily verified by Pawley refinement, because an incorrect unit cell will normally result in significant deviations between the simulated and the experimental powder patterns. In a Pawley refinement, all peak intensities are treated as variable parameters and adjusted together with background parameters, profile parameters, cell parameters, and the zero-point shift of the diffraction pattern to obtain the best possible agreement between a simulated and the experimental diffraction pattern. Pawley refinement proceeds in cycles. In each cycle, the peak intensities and background parameters are optimized first, holding all other parameters fixed. In a second step, the peak intensities and background parameters are kept constant, and the remaining parameters are refined. In the final cycle, all relevant parameters are refined simultaneously.

Space group determination from powder diffraction data is more ambiguous than with single-crystal diffraction, because of the limited number of diffraction peaks and the inability to resolve diffraction peaks with the same interplanar *d* spacing but differing Miller indices. There are several ways to extract space group information from the experimental data. One possible approach is to generate a table of *hkl* indices and intensities to identify systematic absences. This knowledge can be exploited to find possible space groups by using the International Tables for Crystallography.[7] Repeated Pawley refinement in different space groups can also be used to facilitate space group selection. Space groups in which experimentally observed reflections are absent result in high Rwp values and can be discarded. The Rwp value is the weighted Rietveld parameter,[8] and Rwp(w/o bck) is the weighted Rietveld parameter calculated after background subtraction. Of the space groups with low Rwp values, the most likely candidates are those with the smallest number of peaks with vanishing intensity or, in other words, those with the highest number of systematic absences. The space group possibilities can be narrowed down to a number of candidates on the basis of consideration of systematic absences, crystal class and number of molecules in the unit cell, chirality, and space group frequency. If a unique space group cannot be assigned, it may be necessary to carry out calculations on each of the plausible space groups.

Before the structure solution can be attempted in a given space group, a starting model must be created. At this stage, it is necessary to decide the number and type of atoms and ions in the asymmetric unit and to consider the various possibilities to distribute the ions over general and special positions. Knowledge of the unit cell volume and space group, along with a measured density, should allow for the makeup of the asymmetric unit to be determined.[9] To find out how many formula units have to be placed in the asymmetric unit, we initially introduce one formula unit into the asymmetric unit and compare the calculated to the experimental density.

A global optimization algorithm, based on Monte Carlo simulated annealing or Monte Carlo parallel tempering, is used to generate a large number of trial structures. For each trial structure, a powder diffraction pattern is calculated and compared to the experimental data. The similarity between the simulated and the experimental patterns is measured by the weighted Rietveld parameter Rwp. This principle of simulated annealing has been packaged as various software programs[10−12] for structure solution from powder data. The limited number of experimental observations in the powder pattern and the speed of computers both require one to limit the number of variables considered in the problem. The number of variables of the problem can be limited by restraining bond distances and angles of the molecules to known values on the basis of experience with analogous structures. Alternatively, conformations can be calculated using molecular mechanics, semiempirical, or ab initio methods. As a result, seemingly complex molecules can be reduced to a few torsion variables describing the internal degrees of freedom of the molecule, three Cartesian coordinates describing the position of the molecule in the unit cell, and three Eulerian angles describing molecular orientation. In general, during the structure search, the position and orientation of the ions in the asymmetric unit are constantly modified. Ions that consist of several covalently bonded atoms are treated as rigid bodies. Thermal factors are not optimized during the structure search. A single global isotropic thermal factor is used for structure solution, and a value is chosen that is approximately correct for the crystal structure under consideration.

The best crystal structure obtained at the end of several Monte Carlo simulated annealing cycles is not necessarily the correct structure solution. The true crystal structure may have been missed because of an insufficient number of cycles or Monte Carlo step or because the search has not been carried out in the correct space group. It may also happen that structure solution is not possible because the geometries of rigid bodies have not been estimated accurately enough prior to structure solution. To decide whether the crystal structure has been solved, the results of the structure solution procedure are examined carefully. If the lowest Rwp value is obtained in several cycles, one can be fairly confident that the global minimum has been found for the given choice of space group and degrees of freedom.

After structure solution, the accuracy of the crystal structure is further improved by Rietveld refinement.[13] In general, the true evaluation of the correctness of a crystal structure comes from careful inspection of the structural details: bond lengths, bond angles, and anisotropic displacement parameters. In the Rietveld refinement method, most of these parameters are fixed at "chemically reasonable" values to improve the data-to-parameter ratio. As a consequence, it can be difficult to

(4) Boultif, A.; Louer, D. *J. Appl. Crystallogr.* **1991**, *24*, 987.
(5) Shirley, R. A. CRYSFIRE Suite of Programs for Indexing Powder Diffraction Patterns, University of Surrey.
(6) Pawley, G. S. *J. Appl. Crystallogr.* **1981**, *14*, 357.
(7) *International Tables for Crystallography, Volume A*; Hahn, T., Ed.; Kluwer Academic Publishers: Dordrecht, 1989.
(8) Young, R. *The Rietveld Method*; IUCr, Oxford University Press: Oxford, 1995.
(9) Harris, K. D. M.; Tremayne, M.; Kariuki, M. *Angew. Chem., Int. Ed.* **2001**, *40*, 1626.
(10) Engel, G. E.; Wilke, S.; Konig, O.; Harris, K. D. M.; Leusen, F. J. J. *J. Appl. Crystallogr.* **1999**, *32*, 1169.
(11) Pagola, S.; Stephens, P. W. *Mater. Sci. Forum* **2000**, *321*, 40. (Source code and documentation for PSSP are available at http://powder.physics.sunysb.edu).
(12) David, W. I. F.; Shankland, K.; Shankland, N. *Chem. Commun.* **1998**, 931.
(13) Rietveld, H. M. *J. Appl. Crystallogr.* **1993**, 3.

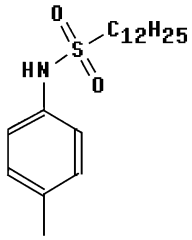

Figure 1. *N*-(*p*-Tolyl)-dodecylsulfonamide molecular structure.

determine the absolute correctness of the structure. There are numerous indications of a correct solution. The most reliable assessment is through the reproducibility of the solution. If multiple solution cycles of the Monte Carlo optimization yield essentially the same solution, the probability of it being the correct solution is much greater. The successful solution of the structure is also confirmed by analysis of its molecular packing. Molecular packing is analyzed to see if any unrealistically close contacts or hydrogen bond patterns exist between adjacent molecules.

Solid-state NMR can assist in the process of structure verification in several ways. The symmetry and multiplicities of the solid-state NMR spectra can place constraints on the number of molecules per asymmetric unit. Chemical shifts can be computed with ab initio methods for multiple molecular conformations. These shifts can be compared to observed ^{13}C chemical shifts to constrain the range of allowed conformations, thus reducing the size of the computation and hence saving time. Furthermore, the same calculations can validate a proposed structure or allow one to select the most likely structure among several alternatives arrived at by the structure solution program. Solid-state NMR is also a very convenient way of detecting solvates and determining their stoichiometry. The title compound, *N*-(*p*-tolyl)-dodecylsulfonamide (see Figure 1), was synthesized at Eastman Kodak Company. This material has an application as an image-enhancement agent in photographic systems.[14] When working with such compounds, it is important to understand crystallization properties. Issues such as polymorphism, milling parameters, unwanted crystallization in coatings, optical properties, solubility, etc., are influenced by the crystal structure of a material. Structure determination of *N*-(*p*-tolyl)-dodecylsulfonamide was undertaken to use the crystal structure as a starting point to understanding the material's properties of this compound. However, repeated attempts to grow single crystals of *N*-(*p*-tolyl)-dodecylsulfonamide were unsuccessful. Therefore, structure elucidation from a polycrystalline sample using powder XRD data was carried out. Additional analyses using computational methods, Monte Carlo simulations and ab initio quantum mechanical calculations, and experimental solid-state NMR were also utilized to validate the derived crystal structure.

Experimental Section

X-ray Powder Data Collection. Initial XRD powder patterns were collected utilizing a Rigaku D2000 Bragg-Brentano diffractometer equipped with a copper rotating anode X-ray source, diffracted beam curved graphite monochromator tuned to Cu Kα radiation (1.54184 Å), and a scintillation detector. The specimen for analysis was prepared by passing an aliquot of the title compound through a 200-mesh sieve and sprinkling the sieved sample onto a zero-background quartz plate.[15] Data were collected using a step scan, 0.01° 2θ/step, 2 s/step. The resulting diffraction pattern is shown in Figure 2.

The data from this pattern show five low-angle diffraction peaks indicative of the first five orders of repeat lattice spacing. These peaks and the peak positions are an indication that there is at least one long axis in the unit cell with a length of ~38.7 Å. Further evaluation of the data in Figure 2 reveals several diffraction peaks in the range of 15−25° 2θ that have acceptable intensity but contain several overlapped peaks. An attempt was made to resolve the peaks and determine the peak positions of the overlapped peaks with a Pearson VII peak profile fitting routine using Jade 6.0 software.[16] The pattern was indexed using DICVOL,[4] and pattern parameters were fitted using a modified Pawley refinement.[10] However, attempts to solve the structure using the laboratory data were unsuccessful. Therefore, it was determined that a high-resolution diffraction pattern would be required to proceed with structure solution.

Synchrotron X-ray diffraction data were collected at Brookhaven National Laboratories on beamline X3B1. The powder diffractometer associated with this beamline is comprised of a Huber goniometer, equipped with a diffracted beam Soller slit assembly with a 0.03° resolution, and a scintillation detector. The wavelength was 1.149642 Å, calibrated using a NIST SRM 1976 α-$A^{l2}O^3$ plate. The specimen for analysis was prepared by passing an aliquot of *N*-(*p*-tolyl)-dodecylsulfonamide powder through a 200-mesh sieve and packing the sieved sample into a 1 mm i.d. glass capillary. Data were collected with the sample spinning, using a step scan, 0.005° 2θ/step, 4 s/step. The resulting diffraction pattern is shown in Figure 3.

The diffraction data in Figure 3 clearly demonstrate the superior quality one can obtain using a synchrotron-based diffractometer for data collection. In particular, the peak resolution and the presence of high-angle 2θ peaks enhance the probability of obtaining a successful indexing solution from powder XRD data.

Structure Solution. Elucidation of the crystal structure from powder XRD data followed a series of steps applied in a systematic approach: (1) unit cell indexing utilizing DICVOL;[4] (2) space group determination based on systematic absences and density considerations; (3) peak profile fitting for peak position and intensity using Pawley refinement;[6] (4) simulated annealing method, independently using PowderSolve[10] and PSSP,[11] for structure determination using a global search algorithm (the solutions obtained from PowderSolve and PSSP were similar; the balance of the work was performed using the solution obtained from PowderSolve); (5) checking and correcting any close atom contacts; and (6) final structure refinement using the Rietveld method.[13]

The powder X-ray diffraction pattern calculated from the refined structure is compared to the synchrotron X-ray diffraction raw data pattern for assessment of correct crystal structure determination. As explained below, comparing the computed and observed molecular properties provided verification of the structure.

Solid-State NMR. High-resolution, solid-state NMR spectra were obtained using a Chemagnetics CMX-300 spectrometer. The spectra were acquired using cross-polarization (CP) and magic angle spinning (MAS) with a contact time of 1 ms and a spinning frquency of 4350 Hz. The nonprotonated carbon signals were assigned using spectral editing based on refocused interrupted decoupling with a dipolar dephasing interval of 80 μs. The results are shown in Figures 4 and 5.

Chemical Shift Calculations. Previous work has shown that ^{13}C chemical shifts computed with quantum mechanics can be useful in

(14) Jain, R.; Schleigh, W. U.S. Patent 5 561 037, 1996.

(15) Gem Dugout, 1652 Princeton Drive, State College, PA 16803.
(16) Jade 6.0, Materials Data Inc., 1224 Concannon Drive, Livermore, CA 94550, 2001.

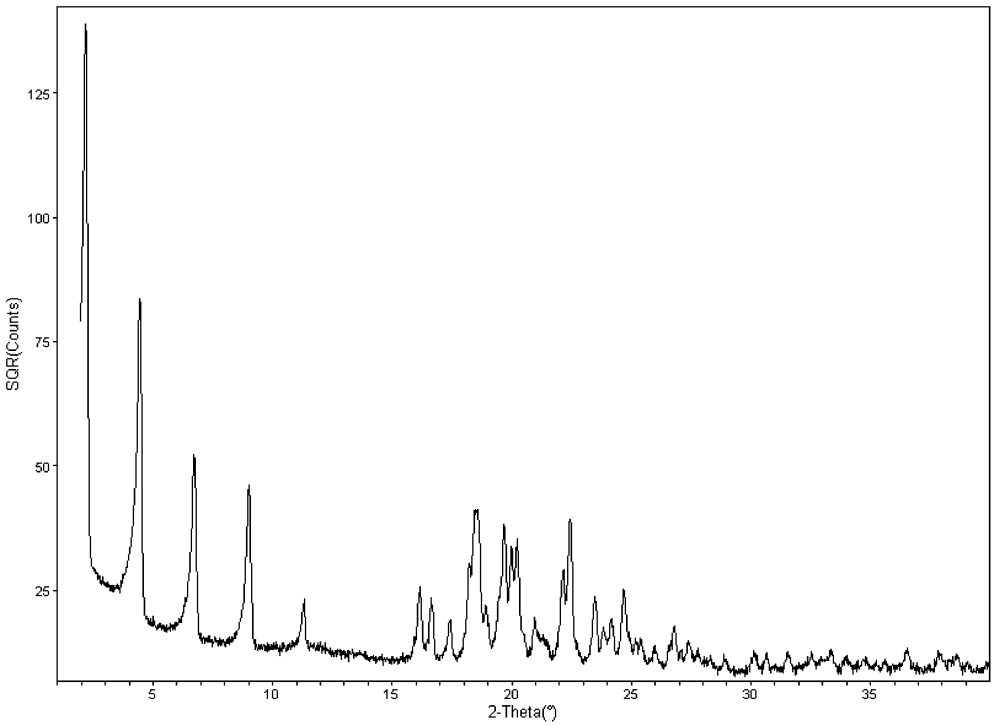

Figure 2. X-ray powder diffraction pattern for *N*-(*p*-tolyl)-dodecylsulfonamide, laboratory source (plotted as square root of intensity to enhance low-intensity diffraction peaks).

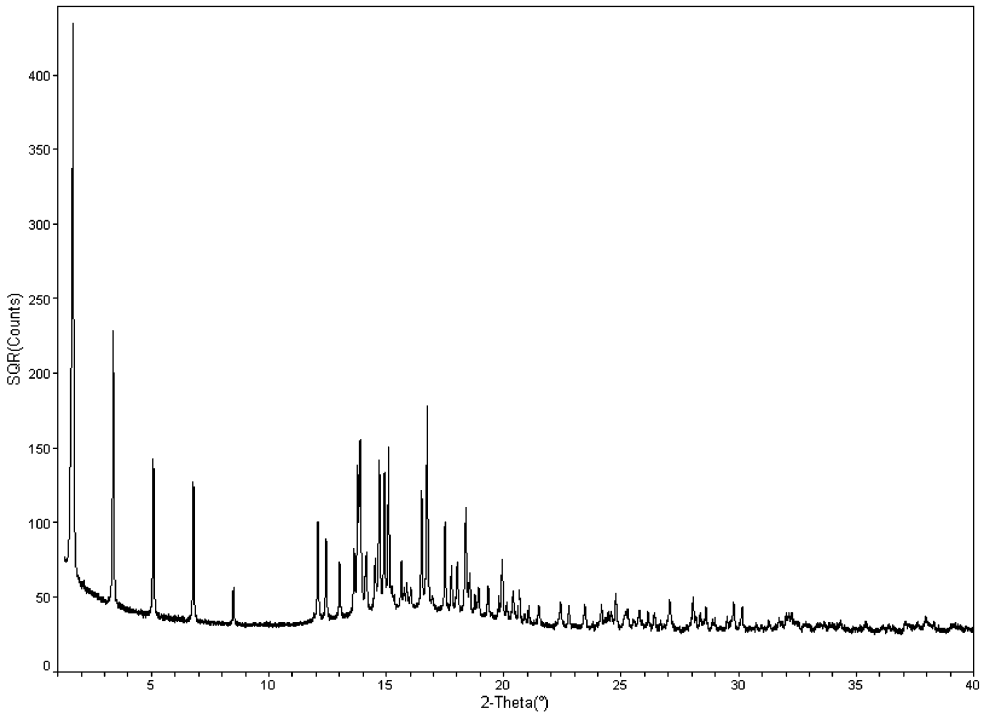

Figure 3. X-ray powder diffraction pattern for *N*-(*p*-tolyl)-dodecylsulfonamide, synchrotron source (plotted as square root of intensity to enhance low-intensity diffraction peaks).

analyzing the solid-state conformations and intermolecular interactions of organic molecules.[17] Gauge-independent atomic orbital (GIAO)[18] NMR ^{13}C shifts were computed using the density functional theory method B3LYP/MIDI!.[19] These quantum mechanical calculations give the absolute chemical shift ($\delta_{absolute}$) of each carbon. These absolute

(17) (a) Ando, S.; Hironaka, T.; Kurosu, H.; Ando, I. *Magn. Reson. Chem.* **2000**, *38*, 241. (b) Havlin, R. H.; Laws, D. D.; Bitter, H.-M. L.; Sanders, L. K.; Sun, H.; Grimley, J. S.; Wemmer, D. E.; Pines, A.; Oldfield, E. *J. Am. Chem. Soc.* **2001**, *123*, 10362. (c) Barich, D. H.; Pugmire, R. J.; Grand, D. M.; Iuliucci, R. J. *J. Phys. Chem. A* **2001**, *105*, 6780. (d) Strohmeier, M.; Orendt, A. M.; Alderman, D. W.; Grant, D. M. *J. Am. Chem. Soc.* **2001**, *123*, 1713.

(18) (a) London, F. *J. Phys. Radium* **1937**, *8*, 397. (b) Schreckenbach, G.; Ziegler, T. *J. Phys. Chem.* **1995**, *99*, 606. (c) Ditchfield, R. *Mol. Phys.* **1974**, *27*, 789. (d) Wolinski, K.; Hinton, J. F.; Pulay, P. *J. Am. Chem. Soc.* **1990**, *112*, 8251.

(19) (a) Becke, A. D. *J. Chem. Phys.* **1993**, *98*, 5648. (b) Stephens, P. J.; Devlin, F. J.; Chabalowski, C. F.; Frisch, M. J. *J. Phys. Chem.* **1994**, *98*, 11623. (c) Easton, R. E.; Giesen, D. J.; Welch, A.; Christopher, J.; Truhlar, D. G. *Theor. Chim. Acta* **1996**, *93*, 281.

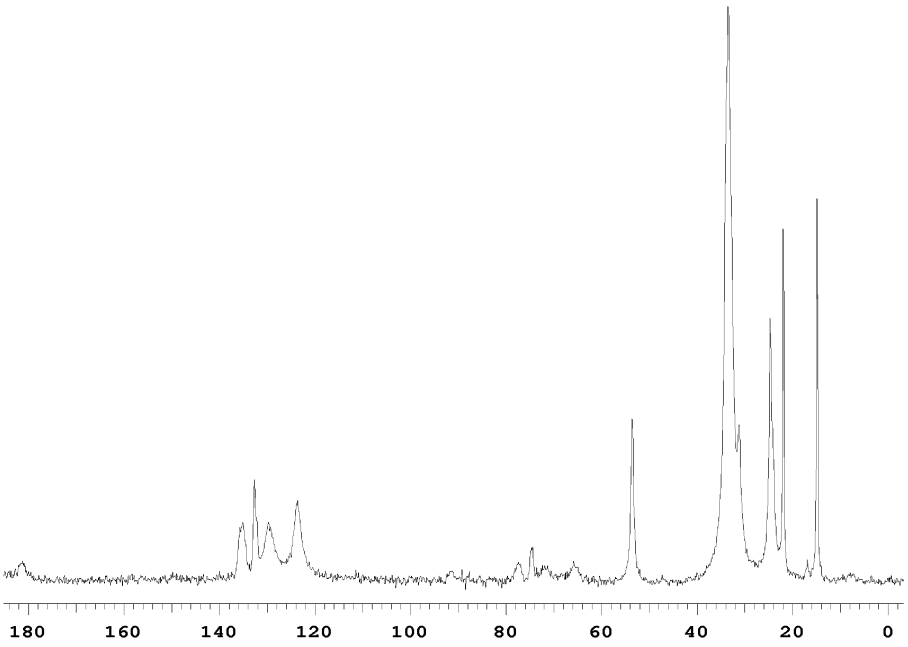

Figure 4. Solid-state ^{13}C CP/MAS NMR spectrum of *N*-(*p*-tolyl)-dodecylsulfonamide.

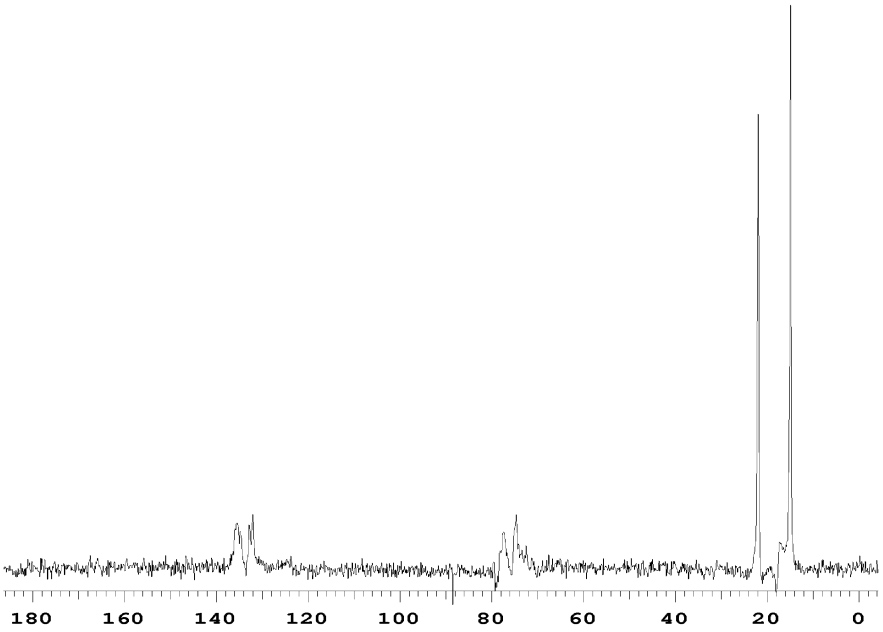

Figure 5. Spectrum edited using the technique of interrupted decoupling. Only nonprotonated aromatic carbons and methyl groups are observed. The peaks between 70 and 80 ppm are spinning sidebands.

shifts can be converted to shifts relative to tetramethylsilane (δ_{Calc}) using a simple slope/intercept equation with general parameters that were developed over a diverse set of 37 organic compounds. These parameters, shown in eq 1, gave an RMS error of 3.6 ppm over the 68 unique carbons in the training set.[20]

$$\delta_{calc} = -1.16*\delta_{absolute} + 225.1 \quad (1)$$

In an extensive comparison of theory and basis set performance using NMR calculations, the B3LYP/MIDI! combination showed better correlation with experiment than other double-ζ basis sets.[20] The most accurate method tested in that paper, B3LYP/6-311+G*, gave only a slight improvement with an RMS error of 2.9 ppm over the 68 carbons in the training set.

All NMR ^{13}C shifts were performed with Gaussian 98.[21]

Results

Powder XRD Structure Determination. The synchrotron X-ray diffraction powder pattern (Figure 3) was indexed as a monoclinic cell with refined lattice constants of $a = 38.773$ Å, $b = 5.507$ Å, $c = 9.509$ Å, and $\beta = 86.35°$. The space group was chosen to be $P2_1/c$ for *N*-(*p*-tolyl)-dodecylsulfonamide, because it had the maximum number of systematic absences

(20) Giesen, D. J.; Zumbulyadis, N. *Phys. Chem. Chem. Phys.* **2002**, *4*, 5498.

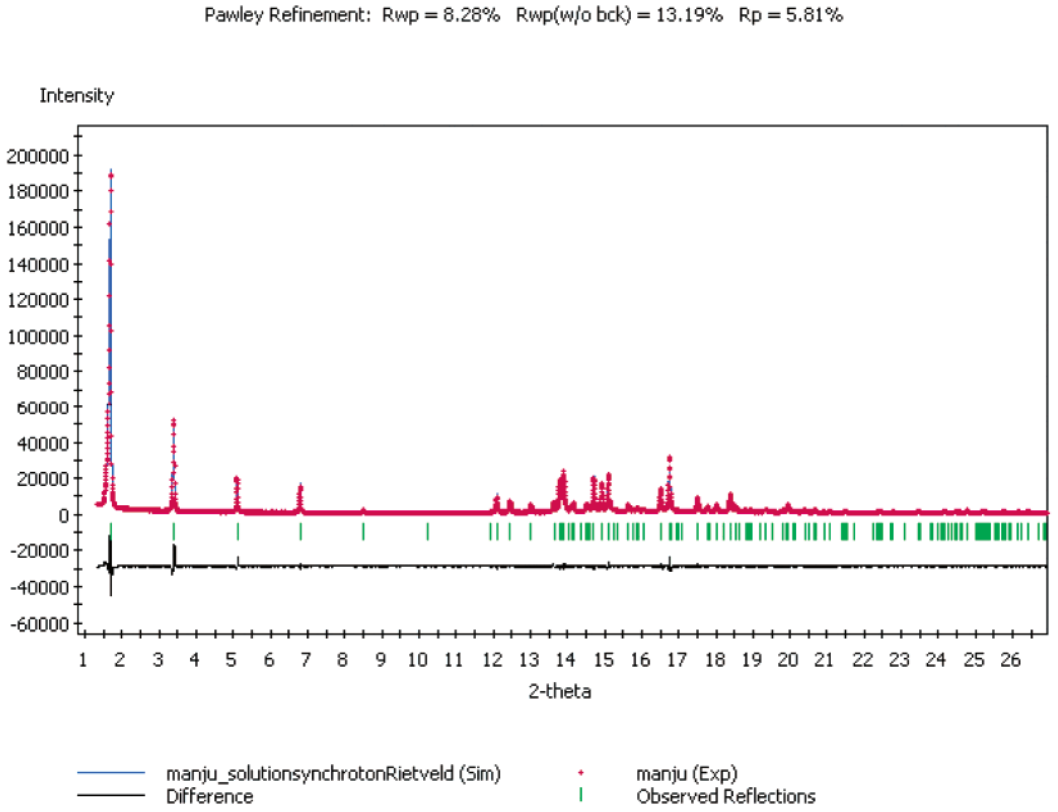

Figure 6. Comparison of diffraction pattern calculated from the indexed unit cell after Pawley refinement (blue) overlaid with the experimental pattern (red). The difference plot (black) is plotted below the overlaid patterns.

compatible with the experimental data. In addition, it has general multiplicity of 4, which provided an acceptable calculated density, and it is the most common space group for organic crystals. Pawley refinement was used to optimize the pattern parameters. The peak profiles were fitted using a pseudo-Voigt function. An asymmetry correction was applied to the first three diffraction peaks by convolution of the profile function with the Finger−Cox−Jephcoat function.[22] The final Pawley refinement Rwp was 8.28% (Figure 6). The parallel tempering method was used as the global search algorithm. Ten independent runs of 30 million Monte Carlo steps starting from different randomly generated points were performed. The best solution (Rwp = 12.39%) was selected as the starting model of the structure. This structure was used for Rietveld refinement. The final optimization of the lattice and pattern parameters by Rietveld refinement resulted in a Rwp of 10.53% (Figure 7). Hydrogen atoms were included in idealized positions.

Structure of *N*-(*p*-Tolyl)-dodecylsulfonamide. Details of the unit cell data are summarized in Table 1. Atomic coordinates and bonding information are listed in Tables 2−5. The bond lengths and bond angles were all fixed at chemically reasonable values. The overall conformation of an *N*-(*p*-tolyl)-dodecylsulfonamide molecule and its atomic numbering scheme are shown in Figure 8. The apparent all-trans, long-alkyl side chain is also confirmed from torsion angles (Table 4). Figure 9 illustrates unit cell packing. Long-range packing in *N*-(*p*-tolyl)-dodecyl-

Table 1. Unit Cell Parameters for *N*-(*p*-Tolyl)-dodecylsulfonamide

empirical formula	$C_{19}H_{33}NO_2S$
formula weight	339.52
wavelength	1.14960 Å
crystal system	monoclinic
space group	$P2_1/c$
unit cell dimensions	$a = 38.773(3)$ Å, $\alpha = 90°$ $b = 5.5066(17)$ Å, $\beta = 86.35(3)°$ $c = 9.509(5)$ Å, $\gamma = 90°$
volume	2026.1(13) Å^3
Z	4
density (calculated)	1.113 Mg/m^3
density (measured)	1.106(8) Mg/m^3

Table 2. Atomic Coordinates ($\times 10^4$) for *N*-(*p*-Tolyl)-dodecylsulfonamide

	x	*y*	*z*		*x*	*y*	*z*
S(1)	1724	−3310	4421	C(13)	2310	−750	3350
O(1)	2010	−4570	5250	C(14)	2480	1680	3030
O(2)	1620	−4510	3170	C(15)	2820	1520	1960
N(1)	1400	−2500	5500	C(16)	2940	4050	1510
C(1)	150	2520	3690	C(17)	3260	3770	700
C(2)	530	1180	4160	C(18)	3390	6120	−100
C(3)	620	−1030	3510	C(19)	3720	6170	−640
C(4)	920	−2210	3940	C(20)	3880	8510	−1440
C(5)	1160	−1330	5070	C(21)	4250	8480	−1980
C(6)	1080	840	5690	C(22)	4360	10 960	−2620
C(7)	750	2030	5210	C(23)	4730	10 860	−3360
C(12)	1940	−420	3800				

(21) Frisch, M. J.; Trucks, G. W.; Schlegel, H. B.; Scuseria, G. E.; Robb, M. A.; Cheeseman, J. R.; Zakrzewski, V. G.; Montgomery, J. A.; Stratmann, R. E.; Burant, J. C.; Dapprich, S.; Millam, J. M.; Daniels, A. D.; Kudin, K. N.; Strain, M. C.; Farkas, O.; Tomasi, J.; Barone, V.; Cossi, M.; Cammi, R.; Mennucci, B.; Pomelli, C.; Adamo, C.; Clifford, S.; Ochterski, J.; Petersson, G. A.; Ayala, P. Y.; Cui, Q.; Morokuma, K.; Malick, D. K.; Rabuck, A. D.; Raghavachari, K.; Foresman, J. B.; Cioslowski, J.; Ortiz, J. V.; Stefanov, B. B.; Liu, G.; Liashenko, A.; Piskorz, P.; Komaromi, I.; Gomperts, R.; Martin, R. L.; Fox, D. J.; Keith, T.; Al-Laham, M. A.; Peng, C. Y.; Nanayakkara, A.; Gonzalez, C.; Challacombe, M.; Gill, P. M. W.; Johnson, B.; Chen, W.; Wong, M. W.; Andres, J. L.; Head-Gordon, M.; Replogle, E. S.; Pople, J. A. *Gaussian 98*, revision A.7; Gaussian, Inc.: Pittsburgh, PA, 1998.
(22) Finger, L. W.; Cox, D. E.; Jephcoat, A. P. *J. Appl. Crystallogr.* **1994**, *27*, 892.

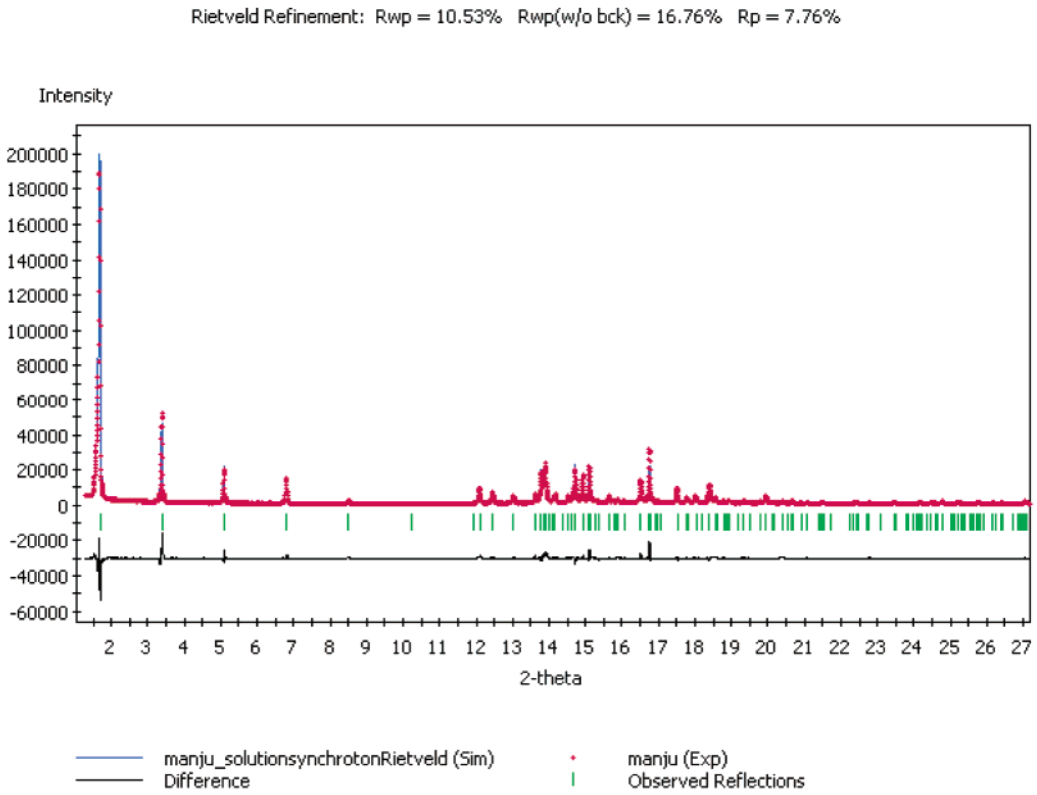

Figure 7. Comparison of diffraction pattern calculated from the structure solution after Rietveld refinement (blue) overlaid with the experimental pattern (red). The difference plot (black) is plotted below the overlaid patterns.

Table 3. Hydrogen Coordinates ($\times 10^4$) for *N*-(*p*-Tolyl)-dodecylsulfonamide

	x	*y*	*z*		*x*	*y*	*z*
H(15)	−100	2200	2700	H(41)	2300	3400	300
H(16)	−300	5600	4000	H(42)	2400	6100	3100
H(17)	200	2400	4000	H(43)	3900	5000	1800
H(18)	100	−2400	2800	H(44)	3100	3300	−300
H(19)	600	−4900	3700	H(45)	3000	7300	−1800
H(20)	1300	2100	7000	H(46)	3300	8800	−400
H(21)	600	3300	6600	H(47)	3900	5200	−100
H(22)	1500	−3500	5700	H(48)	3800	2900	−1800
H(23)	1700	2000	4800	H(49)	3800	7000	−2200
H(24)	2000	−2400	3400	H(50)	3900	11 000	−300
H(25)	2500	−2400	3600	H(51)	4500	7400	−2400
H(26)	2300	−3900	2700	H(52)	3900	9000	−2400
H(28)	2000	4000	4200	H(53)	4200	11 000	−3200
H(29)	2200	2600	2500	H(54)	4700	11 800	−800
H(38)	5100	12 400	−3600	H(55)	5200	9900	−2500
H(39)	3200	−300	2200	H(56)	5100	9600	−4400
H(40)	2900	−600	1900				

Table 4. Torsion Angles [deg] for *N*-(*p*-Tolyl)-dodecylsulfonamide

O(1)−S(1)−N(1)−C(5)	175	C(5)−C(6)−C(7)−C(2)	−3
O(2)−S(1)−N(1)−C(5)	−51	O(1)−S(1)−C(12)−C(13)	39
C(12)−S(1)−N(1)−C(5)	65	O(2)−S(1)−C(12)−C(13)	−85
C(7)−C(2)−C(3)−C(4)	−2	N(1)−S(1)−C(12)−C(13)	154
C(1)−C(2)−C(3)−C(4)	−177	S(1)−C(12)−C(13)−C(14)	−173
C(2)−C(3)−C(4)−C(5)	3	C(12)−C(13)−C(14)−C(15)	−156
C(3)−C(4)−C(5)−N(1)	173	C(13)−C(14)−C(15)−C(16)	171
C(3)−C(4)−C(5)−C(6)	−4	C(14)−C(15)−C(16)−C(17)	174
S(1)−N(1)−C(5)−C(4)	60	C(15)−C(16)−C(17)−C(18)	168
S(1)−N(1)−C(5)−C(6)	−123	C(16)−C(17)−C(18)−C(19)	166
C(4)−C(5)−C(6)−C(7)	4	C(17)−C(18)−C(19)−C(20)	−178
N(1)−C(5)−C(6)−C(7)	−174	C(18)−C(19)−C(20)−C(21)	179
C(3)−C(2)−C(7)−C(6)	2	C(19)−C(20)−C(21)−C(22)	−176
C(1)−C(2)−C(7)−C(6)	177	C(20)−C(21)−C(22)−C(23)	−173

Table 5. Hydrogen Bonds with H··A < *r*(A) + 2.000 Å and ∠DHA > 110°

D–H	*d*(D–H)	*d*(H··A)	∠DHA	*d*(D··A)	A
N1−H22	0.772	1.949	143.42	2.610	O2

sulfonamide, viewed along the *b*-axis, shows *N*-(*p*-tolyl)-dodecylsulfonamide molecules arranged in chains that run parallel to the crystallographic *a*-axis (horizontal in Figure 10). Interactions between chains are primarily alkyl−alkyl on one side and aryl−aryl on the other. One can see a strong intermolecular (1.95 Å) hydrogen bond (Figure 11) between the hydrogen atom of the sulfonamide nitrogen and one of the sulfonic oxygen atoms. Hydrogen bonding information is summarized in Table 5. Materials Studio software by Accelrys[23] was used to generate these diagrams.

NMR Results. The geometry of an *N*-(*p*-tolyl)-dodecylsulfonamide monomer was extracted from the PowderSolve determined structure. The position of the hydrogen atoms was optimized using B3LYP/MIDI!, keeping all other atoms at the determined positions. Using the procedure described above, we computed chemical shifts using this geometry. A comparison of the computed and experimental ^{13}C shifts is given in Table 6. The agreement between experimental and computed shifts is better than the RMS error of 3.6 ppm found when developing the parameters in eq 1; therefore, this result provides further evidence of the validity of the PowderSolve monomer geometry.

Strong intermolecular interactions can sometimes affect ^{13}C NMR shifts, and the PowderSolve-determined structure contains a hydrogen bond between the amine proton on one molecule and an $-SO_2$ oxygen on a neighboring molecule. To check

(23) Accelrys Inc., San Diego, 2002.

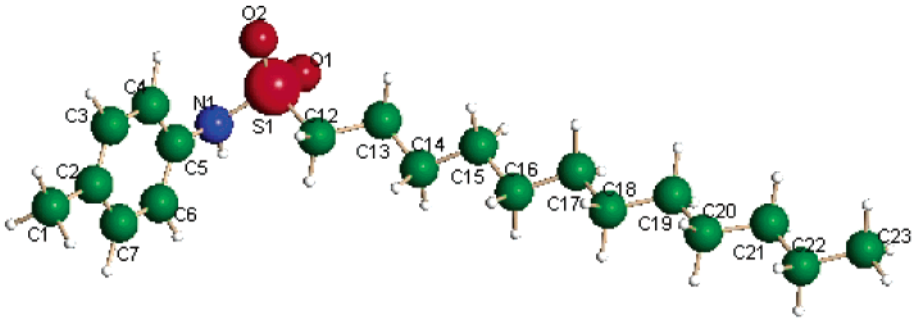

Figure 8. Conformation of *N*-(*p*-tolyl)-dodecylsulfonamide with atomic numbering scheme.

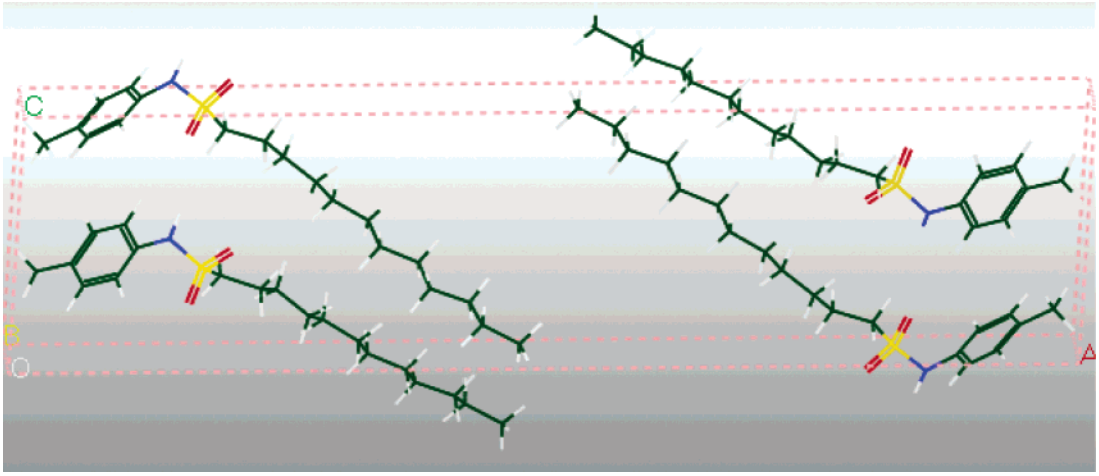

Figure 9. The unit cell packing of the *N*-(*p*-tolyl)-dodecylsulfonamide.

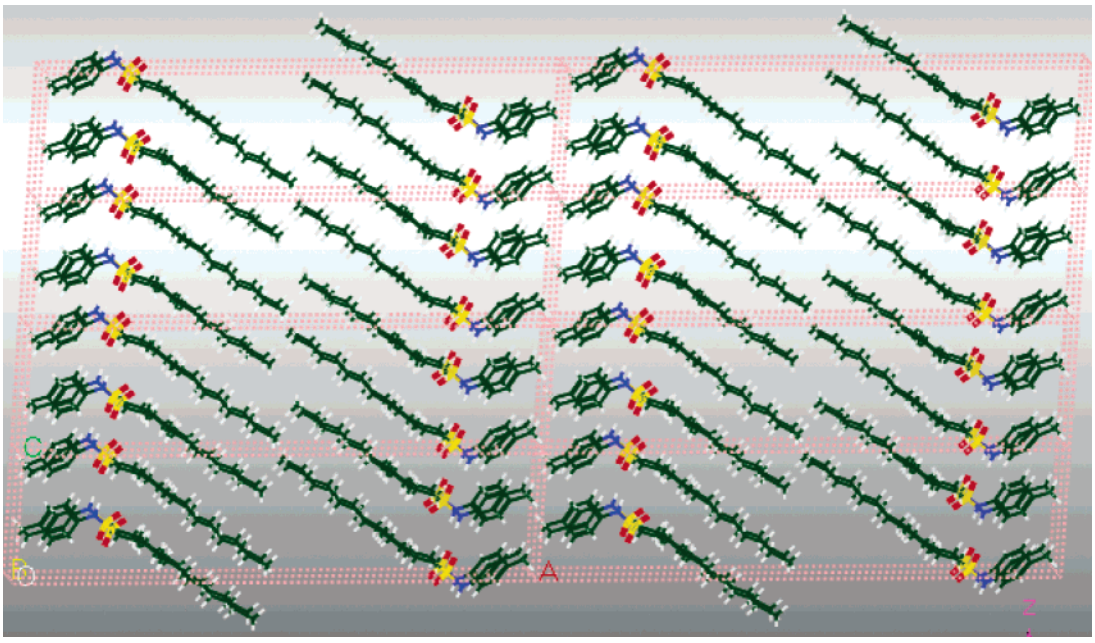

Figure 10. Long-range packing in *N*-(*p*-tolyl)-dodecylsulfonamide, viewed along the *b*-axis.

whether this interaction strongly affects the chemical shifts, the geometry of an *N*-(*p*-tolyl)-dodecylsulfonamide dimer was extracted from the structure. The computed shifts for these molecules were all within 1 ppm of the shifts computed for the monomer structure.

While the computed and experimental shifts in Table 6 are in good agreement, it is possible that other molecular conformations could yield computed shifts much closer to the experimental values. If so, the validity of the simulated annealing results could be in question. If not, it is further confirmation that the results are correct. To resolve this issue, a full potential energy surface was constructed for two important torsions, and at each point ^{13}C shifts were also calculated. The ABCD torsion angle for atoms A, B, C, and D is defined as the angle between the ABC plane and the BCD plane. The two torsions examined are the C(12)SNC(5) torsion and the SNC(5)C(4) torsion.

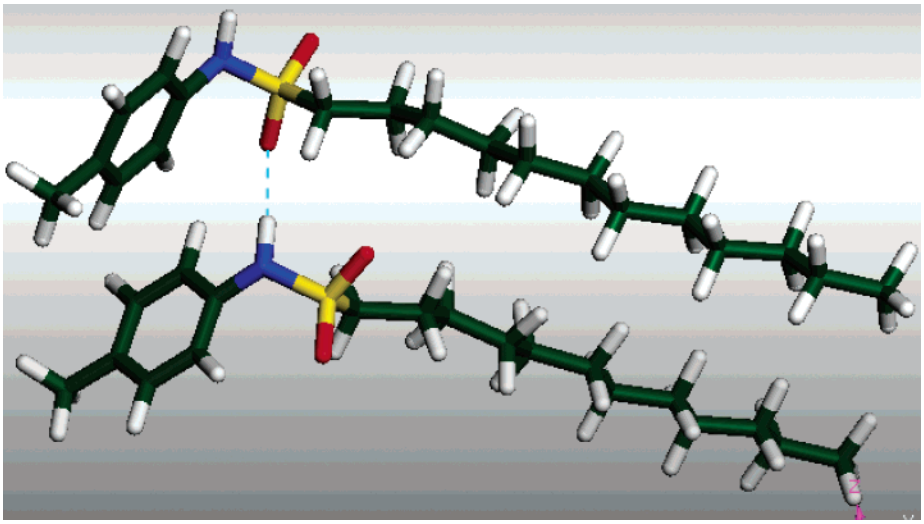

Figure 11. Intermolecular hydrogen bonding in *N*-(*p*-tolyl)-dodecylsulfonamide.

Table 6. Comparison of Experimental Powder NMR^{13}C Shifts and Shifts Computed Using the PowderSolve Geometry

carbon #	experimental	calculated
1	21.9	21
2	132.6	132
3	129.7	132
4	123.6	123
5	135.2	131
6	123.6	123
7	129.7	134
12	53.5	59
13	24.6	23
14	31.2	30
15	33.4	33
16	33.4	31
17	33.4	31
18	33.4	33
19	33.4	32
20	33.4	32
21	33.4	34
22	21.9	24
23	14.8	15

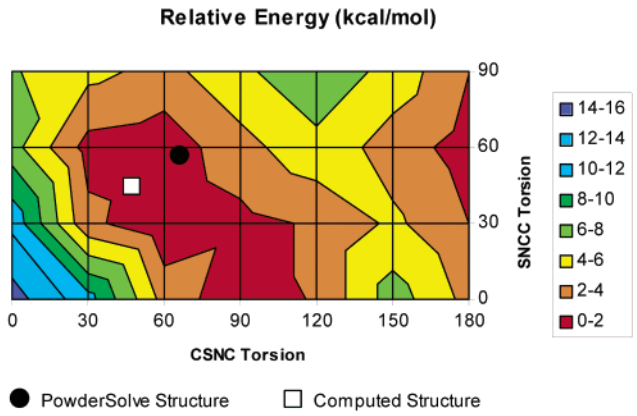

Figure 12. The potential energy surface for twisting about the CSNC and SNCC torsions.

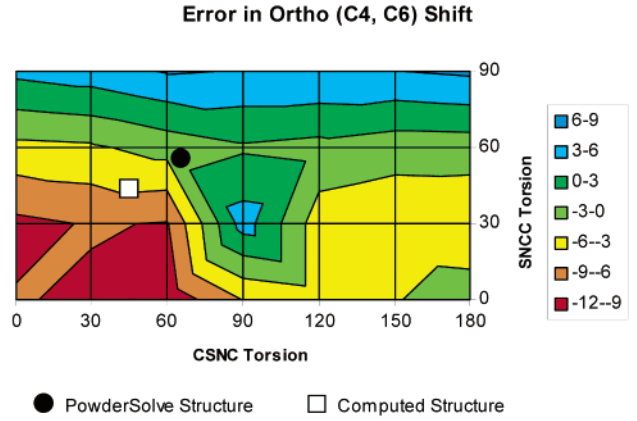

Figure 13. The difference between the average calculated and experimental NMR shifts for C(4) and C(6) as a function of the torsion angles CSNC and SNCC.

Because of the symmetry of the molecule, the CSNC torsion is unique from 0 to 180°, while the SNCC angle is unique only from 0 to 90 because carbon atoms 4 and 6 are identical. For this study, the ballast was truncated at C(14), and all calculations used B3LYP/MIDI! and the G98 computer code.

Figure 12 gives the potential energy surface for rotation about the two torsions. Symbols on the plot give the location of the structure with the minimum computed energy and the structure found by simulated anealing. The two structures are very similar in both torsion angles, and their relative energies are within *RT* (*R* − gas constant, *T* − temperature) at room temperature.

The chemical shifts of carbon atoms 2, 4, and 6 in the phenyl ring were the most sensitive to the CSNC and SNCC torsion angles. The error relative to experiment for carbon atoms 4 and 6 at each set of torsion angles is given in Figure 13. Because the two carbons are equivalent on the NMR time scale, the average of the computed shifts was used for this comparison. The average shift calculated with the PowderSolve structure is closer to experiment than the average shift calculated at the minimum energy structure. Because the shift for this carbon is so sensitive to the two torsions, and the calculations with the proposed structure agree within 1 ppm with experiment, it is likely that the proposed structure is close to the actual structure.

The chemical shift for the para carbon (C(2)) is also somewhat sensitive to the position of the two torsions. The difference between calculated and experiment at each set of torsions is given in Figure 14. The shifts from both the simulated annealing and the minimum energy structure lie in regions of good agreement with experiment, again demonstrating that the structure is reasonable. Taken together, the results from the computations support the final proposed structure. This structure

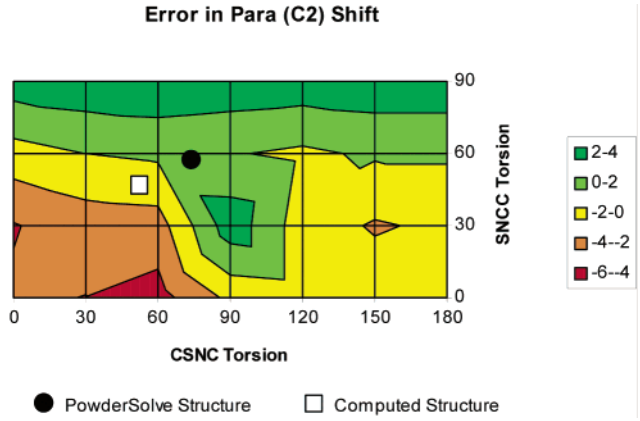

Figure 14. The difference between the calculated and experimental NMR shift for C(2) as a function of the torsion angles CSNC and SNCC.

is geometrically and energetically similar to the minimum energy structure. The ^{13}C shifts calculated for the monomer, and when including intermolecular interactions, are quite close to the experimental values, particularly for those carbons that are sensitive to conformational changes.

Discussion and Conclusions

In this paper, we have demonstrated the feasibility of an integrated approach to the determination and verification of a complete 3-D structure for a medium-sized organic molecule. Our approach uses a combination of powder XRD data, several computational packages involving Monte Carlo simulations and ab initio quantum mechanical calculations, and experimental solid-state NMR chemical shifts. The primary benefit of this approach is that it allows for structure elucidation when single crystals are unavailable or difficult to procure. As an ancillary benefit, the calculations can serve as the starting point for the determination of conformation in solution and for the computation of other spectroscopic and optical properties.

Experience to date suggests the following workflow for crystal structure determination from polycrystalline materials:

(1) Collect powder XRD patterns utilizing a laboratory X-ray source to assess the crystalline nature of the material and to assess the phase composition.

(2) Obtain and assign solid-state NMR data concurrently with the collection of powder XRD data to detect the possible presence of solvates, ascertain morphological purity (absence of coexisting polymorphs), and, in some cases, determine the number of molecules per asymmetric unit.

(3) Confirm the chemical stoichiometry using elemental analysis. Measure the density of the sample to get an assessment of the number of molecules (Z) in the asymmetric unit. The value for Z is calculated from knowledge of the molecular weight, unit cell volume, and measured density. As a check on structure correctness, compare the measured density and calculated X-ray density.

(4) Proceed with the crystallographic computations using a simulated annealing software package, once powder XRD data of satisfactory quality and correct unit cell indexing have been obtained. Computed geometries can be used as a starting point and to lock in certain geometric coordinates.

(5) Validate the computed structure by calculating ab initio its solid-state NMR spectrum and comparing it to experimental observations. Alternatively, use the ab initio calculations to select the most likely among several computed structures.

The three-dimensional structure and packing of molecules in the solid state is crucial in the optimization of many technologically useful materials properties. Significant among them are the stability of the vitreous state and the inhibition of crystallization. This stability is important in the case of dispersions used in conventional sensitized products, as well as in advanced electrooptical devices such as organic light-emitting diodes. Packing and aggregation phenomena in solution and the solid state determine the optical and photochemical properties responsible for image quality and stability.

Acknowledgment. The authors wish to thank Al Mura for providing *N*-(*p*-tolyl)-dodecylsulfonamide samples, Anne Marie Lanzafame for recrystallization activities, and Craig Barnes for assistance in data collection, all of Eastman Kodak Company Research was carried out in part at the National Synchrotron Light Source at Brookhaven National Laboratory, which is supported by the U.S. Department of Energy, Division of Materials Sciences and Division of Chemical Sciences. The SUNY X3 beamline at NSLS is supported by the Division of Basic Energy Sciences of the U.S. Department of Energy (DE-FG02-86ER45231).

JA027978B